**Supplementary data**



2
**Supplemental Figure 1 (Related to Figure 1). Loss of lymphatic vessels in lung allograft**
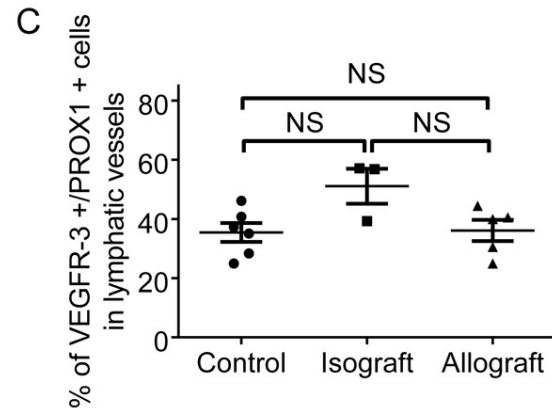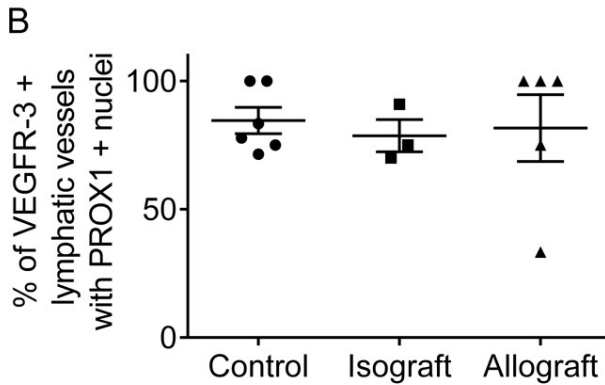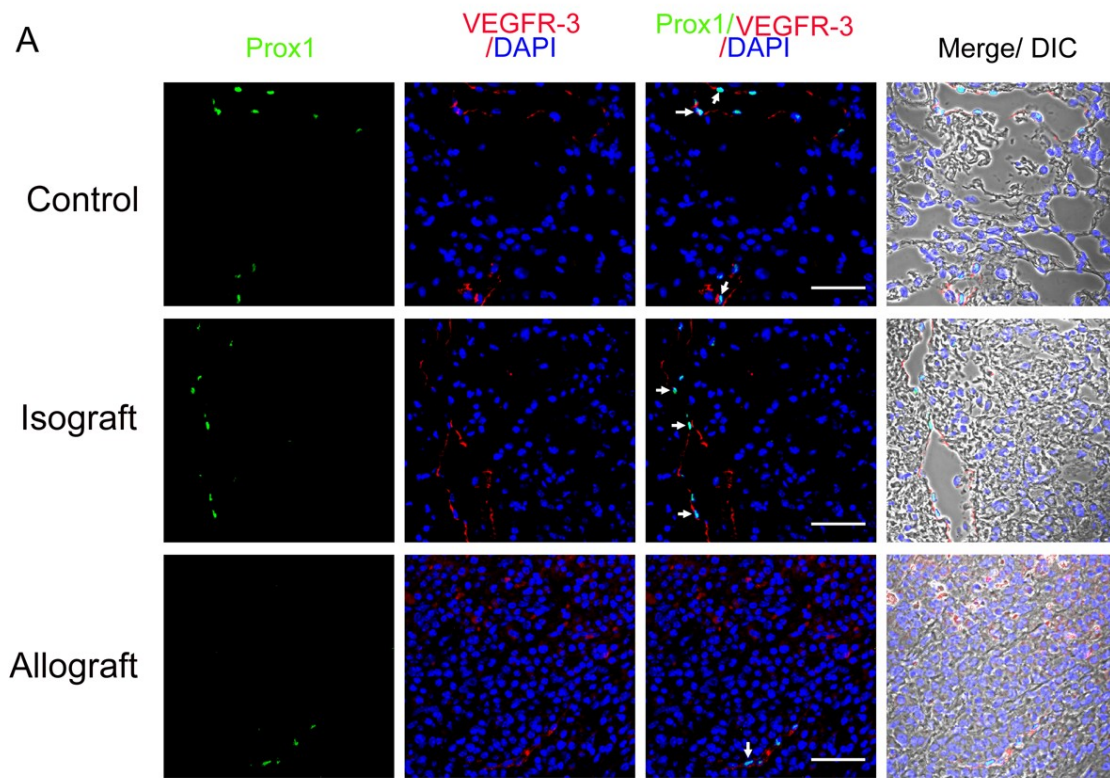**rejection.** (**A and B**) Representative images of H&E staining (**A**) and LYVE-1
immunohistochemical staining (**B**) of control untransplanted lungs (n=6 mice), isografts (n=3
mice) and allografts (n=5 mice) shown at low magnification (upper panels) and high
magnification (lower panels). LYVE-1-positive lymphatic vessels are indicated by black arrows.
The areas enclosed in the rectangles in the upper panels are enlarged in the lower panels. Scale
bars, 200μm. Animals receiving isogeneic or allogeneic lung grafts were sacrificed 30 days after
transplant together with age-matched untransplanted controls.
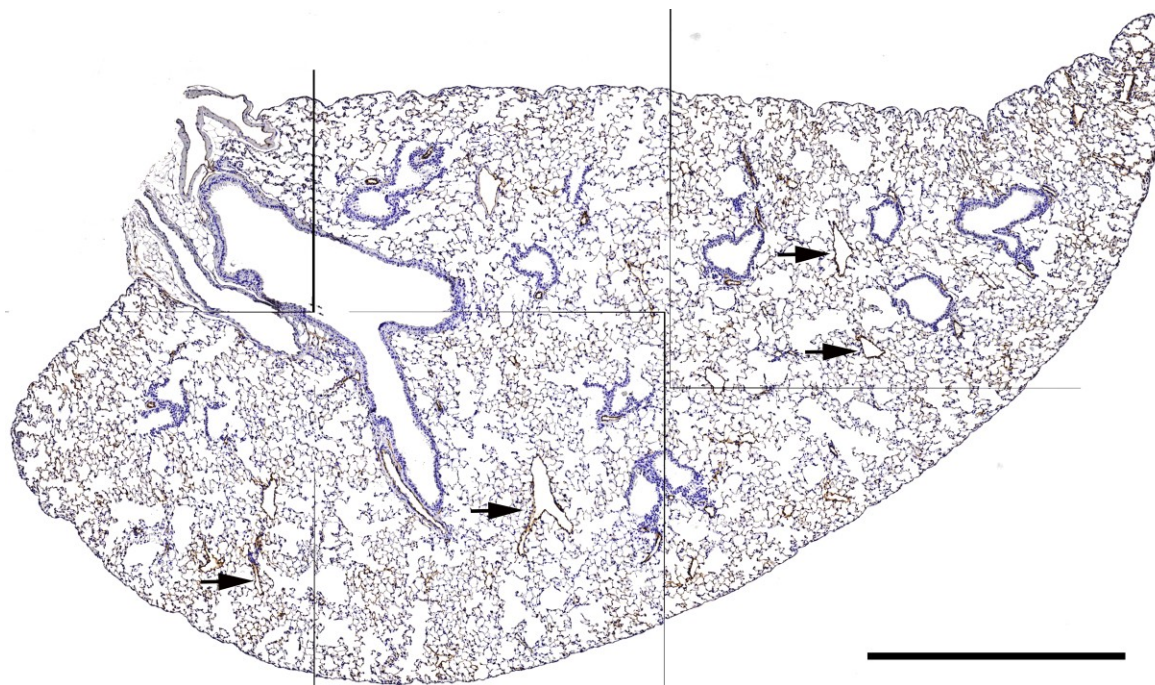
**Supplemental Figure 2. Representative digitally reconstructed image of LYVE-1 immunohistochemical staining of a control mouse lung.** Multiple photomicrographs of LYVE-1 immunohistochemical staining were captured and aligned to generate panoramic images of entire tissue sections. The number of LYVE-1-positive lymphatic vessels (indicated by black arrows) were quantified and subsequently adjusted to the cross sectional area of the entire tissue. Scale bar, 1000 μm.

**Supplemental Figure 3 (Related to Figure 1). Double immunofluorescence staining verifies the loss of lymphatic vessels in lung allograft rejection.** (**A**) Representative images of double immunofluorescence staining with anti-PROX-1 (green) and anti-VEGFR-3 (red) antibodies in lung tissues from control untransplanted lungs (n=6 mice), isografts (n=3 mice) and allografts (n=5 mice). Nuclei were counterstained with 4',6-diamidino-2-phenylindole (DAPI, blue). PROX-1/VEGFR-3 double positive cells are indicated by white arrows. Scale bars, 50μm. (**B**) Percentage of VEGF-R3-positive lymphatic vessels with PROX1-positve nuclei. (**C**) Percentage of VEGFR-3/Prox-1-double positive cells in lymphatic vessels. All data were presented as mean ± SEM. There were no statistically significant differences between groups as determined by 1-way ANOVA.
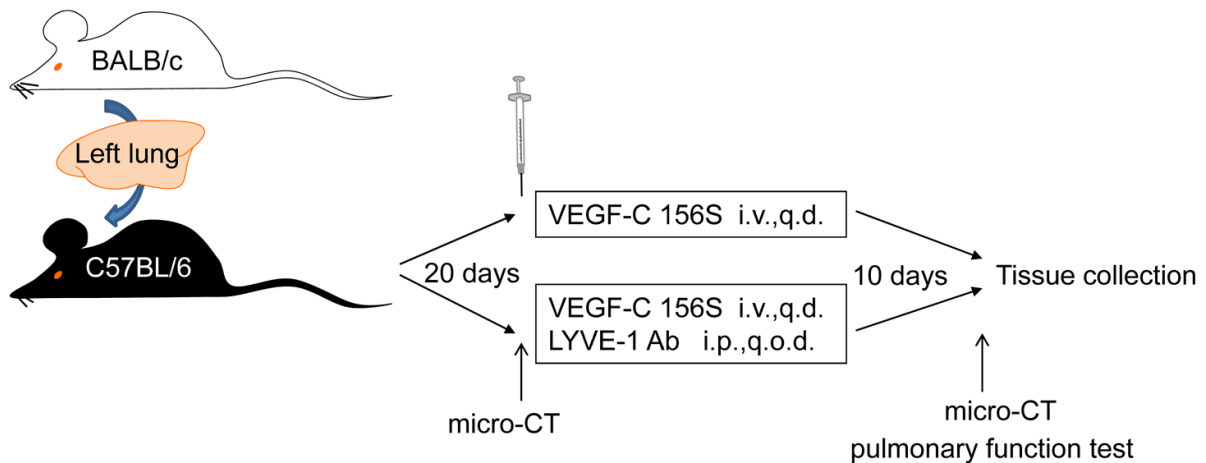
1
2
3
4
5
6
7
8  **Supplemental Figure 4. Schematic depicting the experimental design.** Orthotopic left lung
9  transplants were performed (BALB/c donor to fully MHC-mismatched C57BL/6 recipient). The
10 involvement of lymphatic vessels in lung allograft function and survival was determined by
11 therapeutically administrating VEGF-C156S to animals through daily intravenous injection (i.v.)
12 after the onset of acute allograft rejection. Meanwhile, the exact roles of lymphatic vessels in
13 transplant pathophysiology was further explored through a parallel loss-of-function experiment
14 in which a group of VEGF-C156S treated allograft recipients were co-treated with LYVE-1
15 function blocking antibodies through intraperitoneal injection (i.p.) every other day. Mice were
16 injected from day 20 post-transplant until sacrifice at day 30. In vivo imaging of mouse lung was
17 performed at day 20 and day 30 using a μCT scanner. Peak airway pressure was measured at the
18 end of the study to evaluate lung function.
19
20
21
22
23
24
25
26
27
28
29
30
31
32
33

Control      PBS      VEGF-C      VEGF-C + LYVE-1Ab
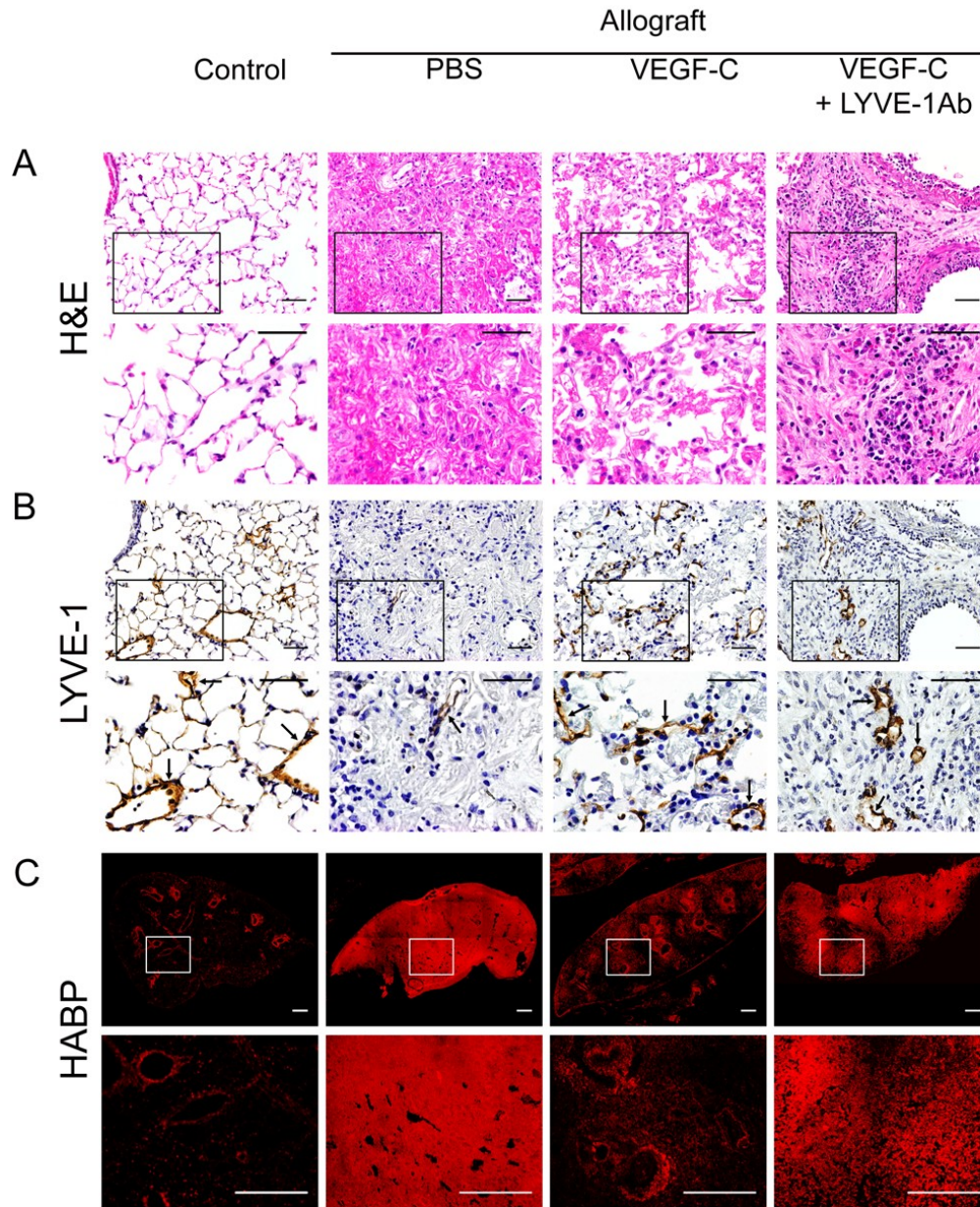
Allograft

**Supplemental Figure 5 (Related to Figure 2). VEGF-C156S treatment ameliorates lung allograft rejection by clearing hyaluronan.** (**A** and **B**) Representative images of H&E (**A**) and LYVE-1 (**B**) staining shown at low magnification (upper panels) and high magnification (lower panels). LYVE-1-positive lymphatic vessels are indicated by black arrows. Scale bars, 50μm. (**C**) Representative images of hyaluronic acid binding protein (HABP) fluorescent staining (red). Scale bars, 500μm. (**A-C**) The areas enclosed in the rectangles in the upper panels are enlarged in the lower panels. Animals receiving allogeneic lung grafts were treated with PBS (n=5 mice), VEGF-C156S (VEGF-C) (n=6 mice) or concomitantly treated with VEGF-C156S and LYVE-1 function blocking antibody (VEGF-C+LYVE-1 Ab) (n=6 mice) from day 20 to day 30 after transplant. Age-matched untransplanted animals were used as controls (n=6 mice).
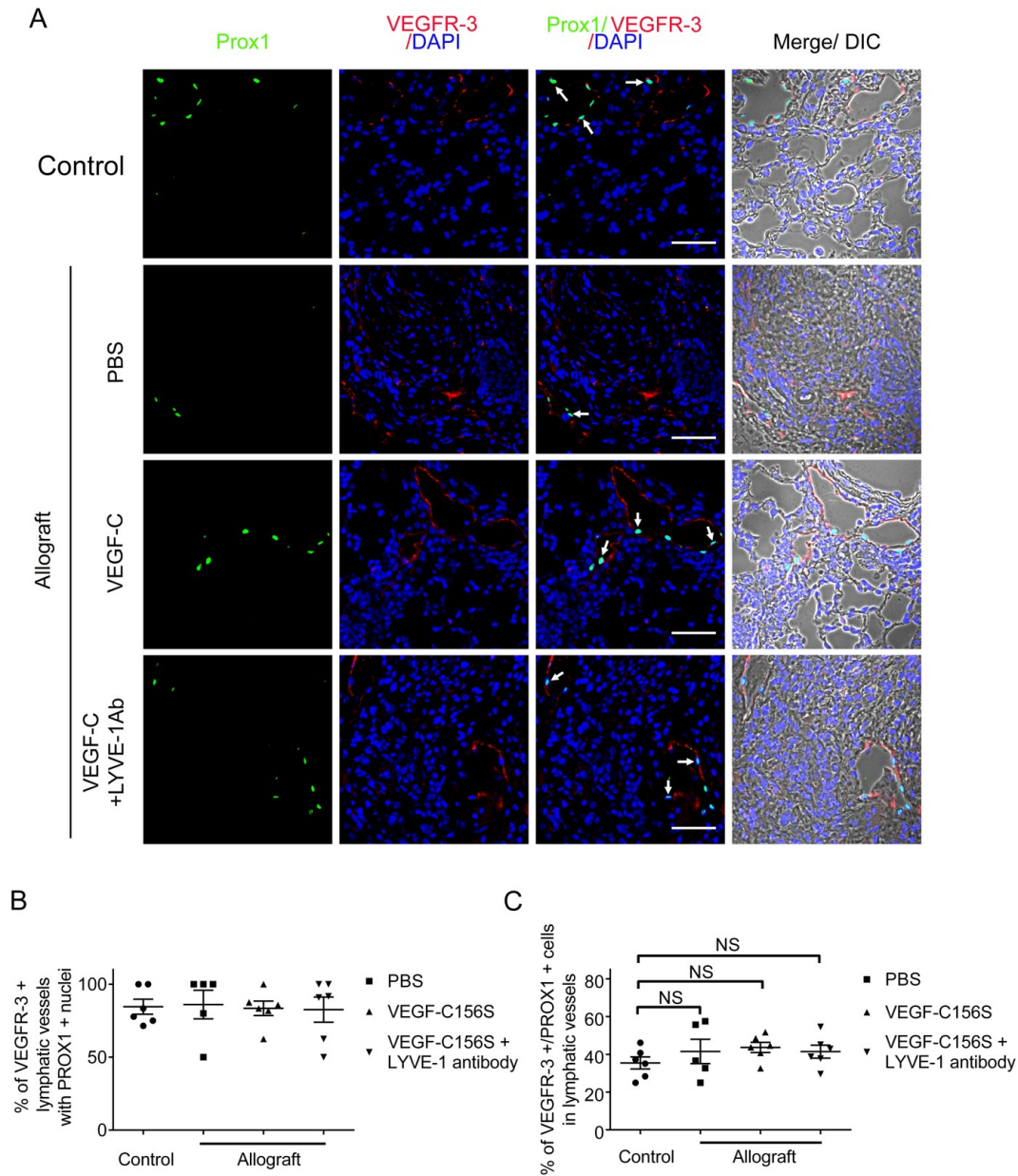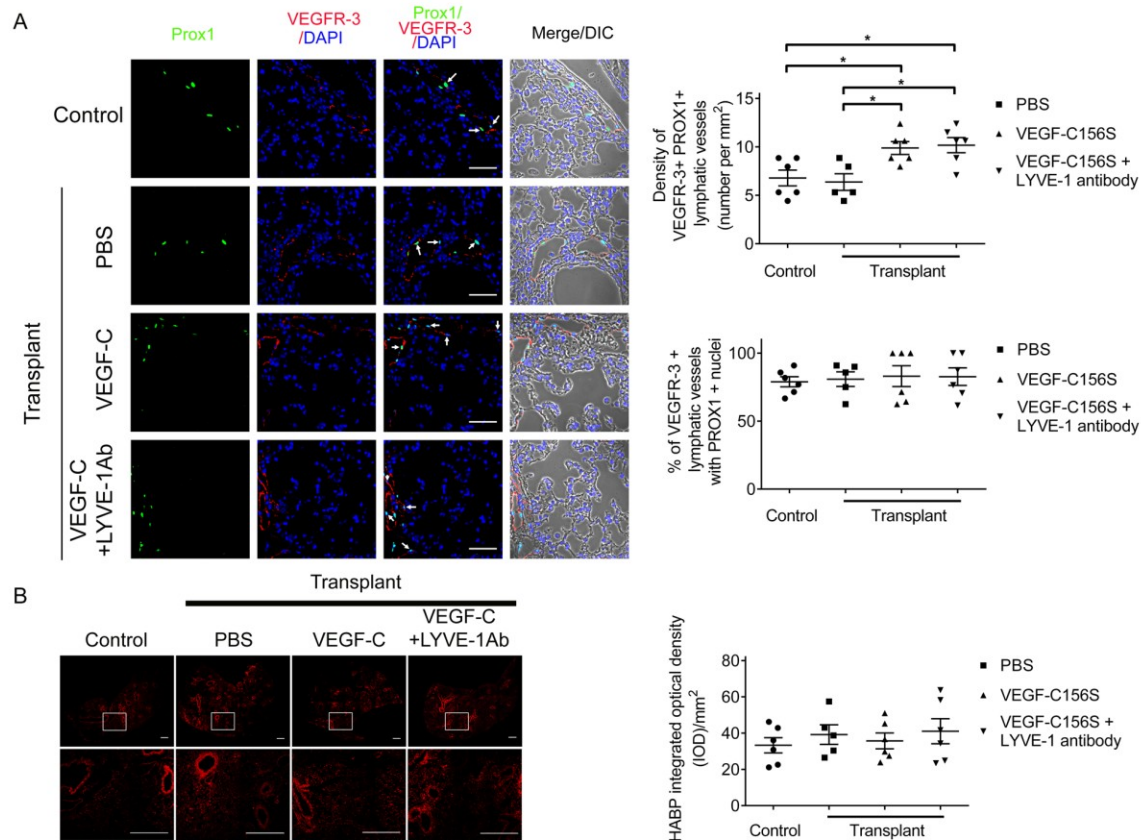
**Supplemental Figure 6 (Related to Figure 2). Double immunofluorescence staining verifies the pro-lymphangiogenic effects of VEGF-C156S treatment.** (**A**) representative images of double immunofluorescence staining with anti-PROX-1 (green) and anti-VEGFR-3 (red) antibodies in mouse left lung. PROX-1/VEGFR-3 double positive cells are indicated by white arrows. Nuclei were counterstained with DAPI (blue). Scale bars, 50µm. Animals receiving allogeneic lung grafts were treated with PBS (n=5), VEGF-C156S (VEGF-C) (n=6 mice) or VEGF-C156S and LYVE-1 function blocking antibody (VEGF-C+LYVE-1 Ab) (n=6) from day 20 to day 30 after transplant. Untransplanted animals were used as controls (n=6). (**B**) Percentage of VEGF-R3-positive lymphatic vessels with PROX1-positve nuclei. (**C**) Percentage of VEGFR-3/Prox-1-double positive cells in lymphatic vessels. Data were presented as mean ± SEM. No statistically significant differences by 1-way ANOVA.
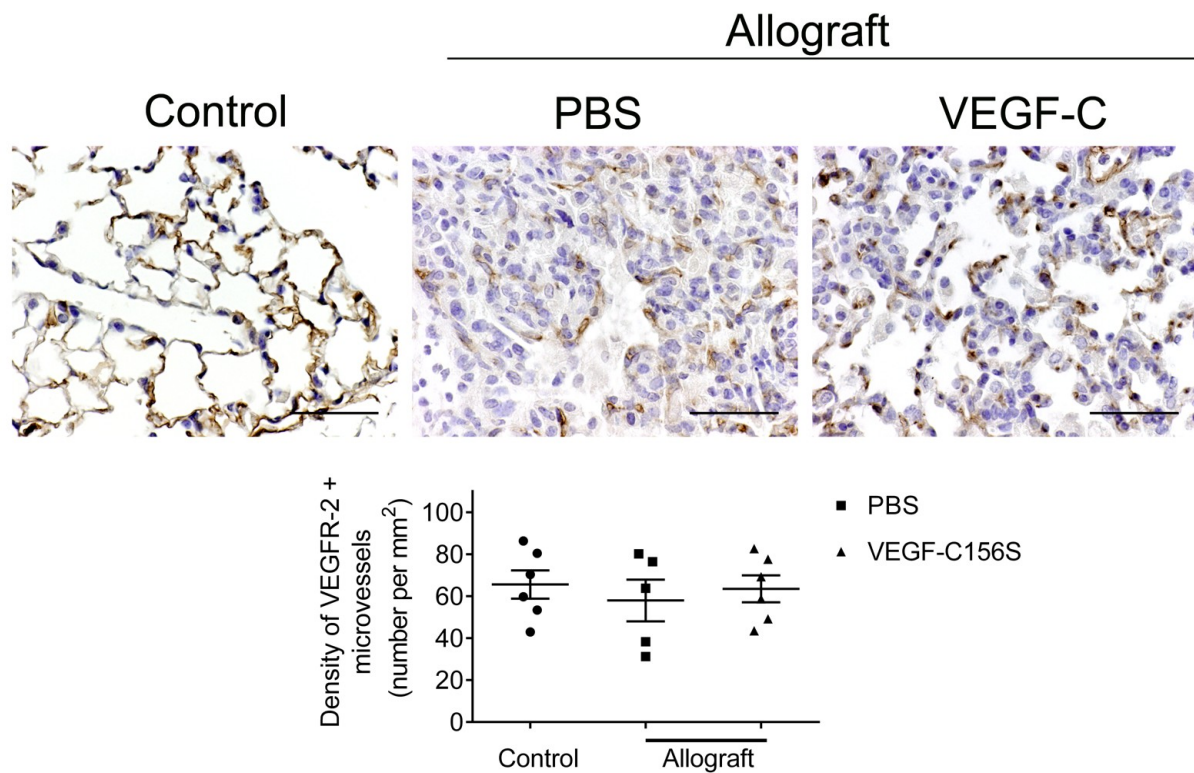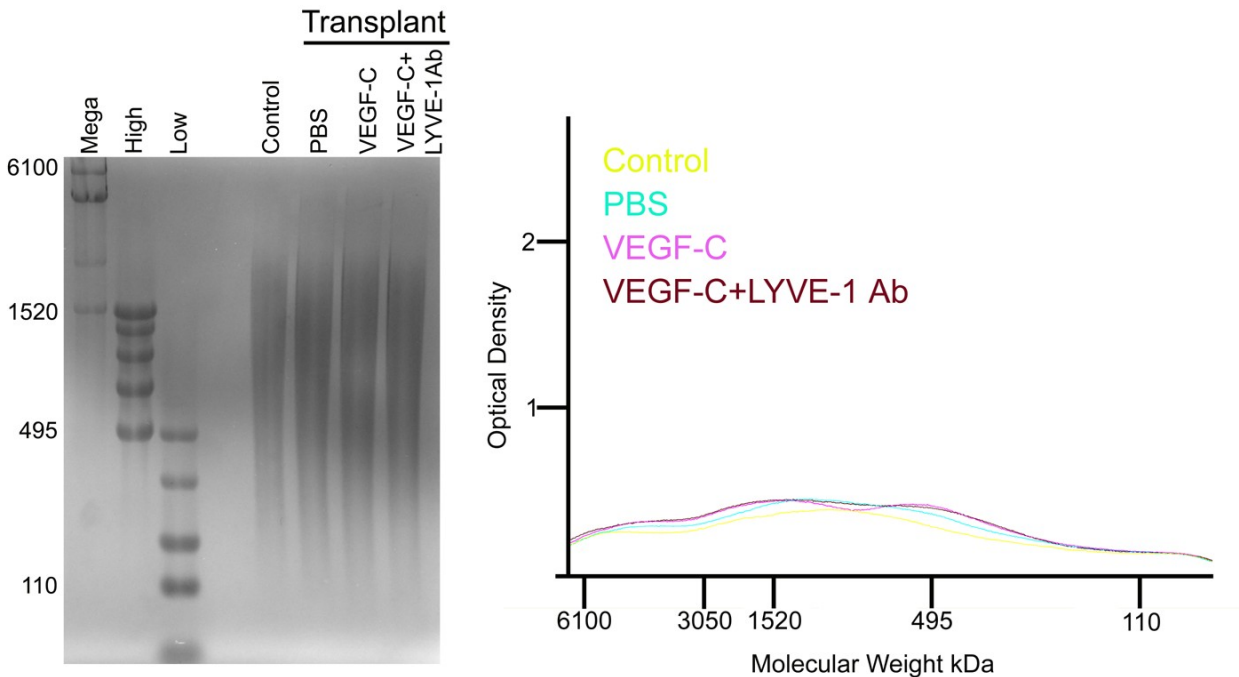
**Supplemental Figure 7. VEGF-C 156S treatment does not affect blood vessel density.** Upper panel: representative images of VEGFR-2 immunohistochemical staining of control untransplanted lungs and allografts treated with either PBS or VEGF-C156S. Scale bars, 50μm. Lower panel: images of the entire lung section were obtained. The number of VEGFR-2-positive blood vessels were quantified and subsequently adjusted to the cross sectional area of the entire tissue. Animals receiving allogeneic lung grafts were treated with PBS (n=5 mice) or VEGF-C156S (VEGF-C) (n=6 mice) from day 20 and sacrificed 30 days after transplant together with age-matched untransplanted controls (n=6 mice). All data were presented as mean ± SEM. There were no statistically significant differences between groups as determined by 1-way ANOVA.

**Hyaluronidase**

Before    After
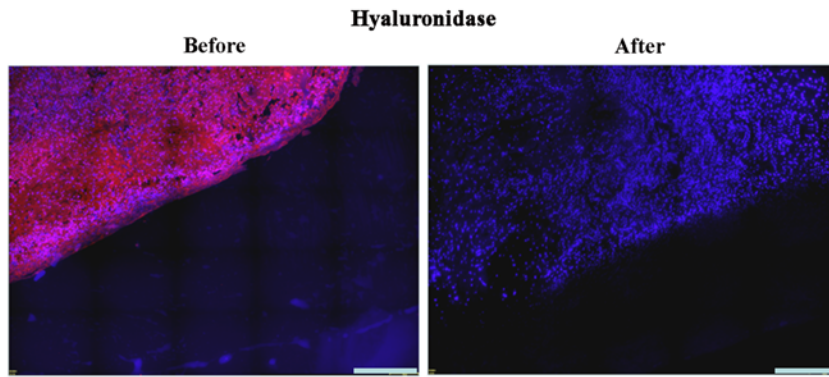
**Supplemental Figure 8. Specificity of hyaluronan binding protein is confirmed by pre-treatment with hyaluronidase.** Hyaluronidase pretreatment abolished hyaluronic acid reactivity (red) in allograft tissue sections, which confirmed the specificity HABP staining. Nuclei were counterstained with DAPI (blue). Scale bars, 200μm.

1
2

A

Prox1 | VEGFR-3/DAPI | Prox1/VEGFR-3/DAPI | Merge/DIC

Control

Transplant — PBS, VEGF-C, VEGF-C+LYVE-1Ab

Transplant

B

Control | PBS | VEGF-C | VEGF-C+LYVE-1Ab

Transplant

3
4 **Supplemental Figure 9. VEGF-C156S treatment induces lymphangiogenesis but does not**
5 **affect HA deposition in native right lungs.** (**A**) Left panel: representative images of double
6 immunofluorescence staining with anti-PROX-1 (green) and anti-VEGFR-3 (red) antibodies in
7 right lung. PROX-1/VEGFR-3 double positive cells are indicated by white arrows. Nuclei were
8 counterstained with DAPI (blue). Scale bars, 50μm. Upper-right panel: quantification of
9 lymphatic vessel density in right lungs. Lower-right panel: percentage of VEGF-R3-positive
10 lymphatic vessels with PROX1-positive nuclei in right lungs. (**B**) Representative images of
11 HABP fluorescent staining (red) in right lungs (left panel) and quantification of HABP integrated
12 optical intensity (IOD) (right panel). Scale bars, 500μm. Areas enclosed in the upper panel are
13 enlarged in the lower panel. Animals were treated with PBS (n=5), VEGF-C156S (VEGF-C)
14 (n=6) or VEGF-C156S and LYVE-1 function blocking antibody (VEGF-C+LYVE-1 Ab) (n=6)
15 from day 20 to day 30 after left lung transplant. Untransplanted animals were used as controls
16 (n=6). All data were presented as mean ± SEM. *$p<0.05$, as determined by 1-way ANOVA.

17
18
19
20
21
22
23

1
2



3
**Supplemental Figure 10. VEGF-C156S treatment does not affect HA molecular mass in native right lungs.** Left panel: agarose gel electrophoresis was conducted to analyze HA size in native right lungs. From left to right: Mega (6100, 4570, 3050, 1520kDa), high (1510, 1090, 966, 572, 495kDa) and low (495, 310, 214, 110, 27kDa) HA ladders were used to determine the molecular mass of HA tissue samples. HA samples per lane were pooled from the upper portions of native right lungs in each group. Right panel: quantitative analysis of HA profiles in mouse native right lungs. Animals receiving allogeneic left lung grafts were treated with PBS (n=5 mice), VEGF-C156S (VEGF-C) (n=6 mice) or concomitantly treated with VEGF-C156S and LYVE-1 function blocking antibody (VEGF-C+LYVE-1 Ab) (n=6 mice) from day 20 to day 30 after transplant. Age-matched untransplanted animals were used as controls (n=6 mice).

14
15
16
17
18
19
20
21
22
23
24
25
26
27
28
29
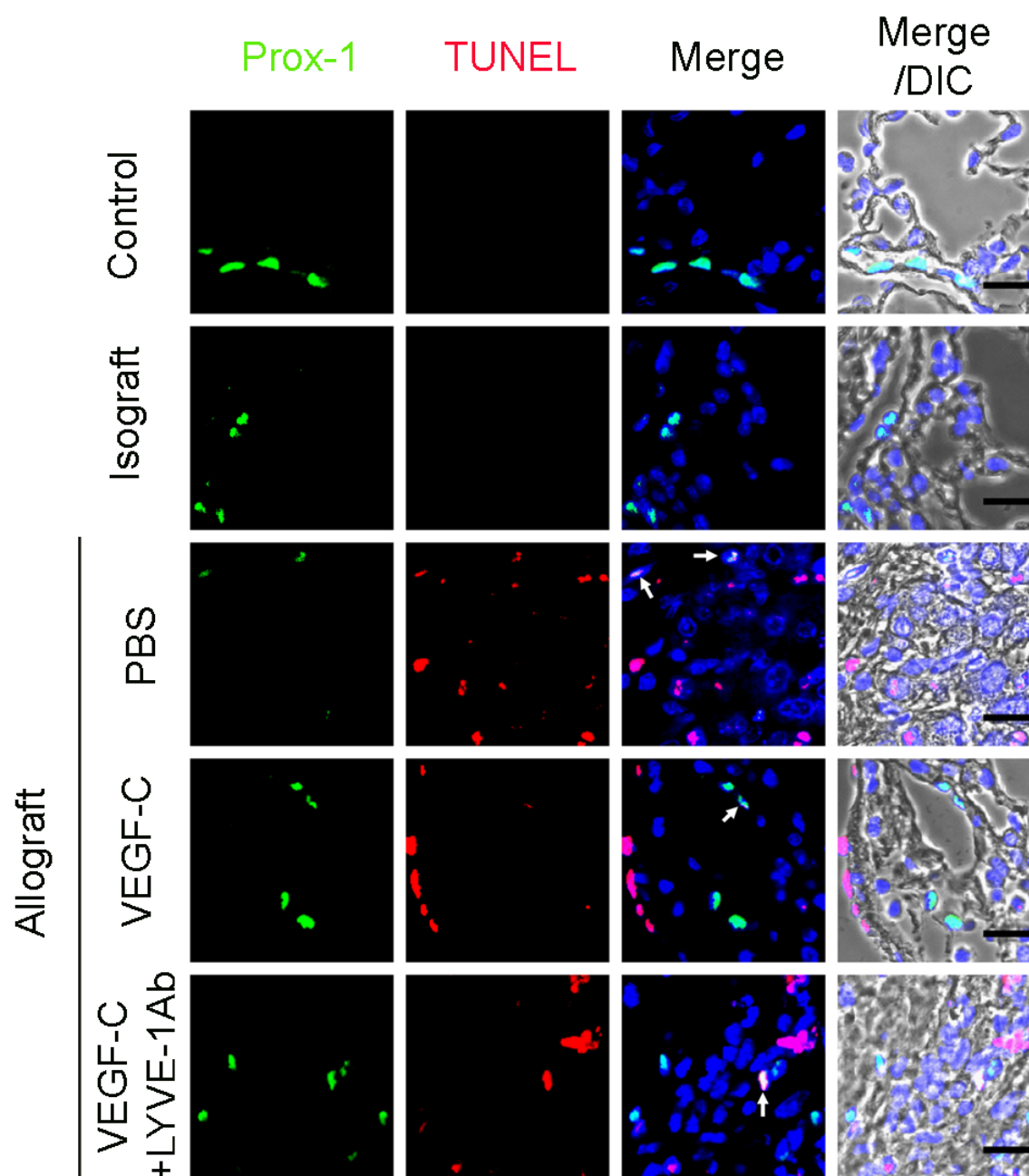
Supplemental Figure 11 (higher magnification of images in Figure 4). VEGF-C156S
treatment reduces lymphatic endothelial cell apoptosis in lung allografts. Representative
images of PROX1 (green) and terminal deoxynucleotidyl transferase-mediated dUTP nick-end
labeling (TUNEL, red) double immunofluorescence staining. PROX-1/TUNEL-double positive
cells are indicated by white arrows. Nuclei were counterstained with DAPI (blue). Scale bars,
20μm. Animals receiving allogeneic lung grafts were treated with PBS (n=5 mice), VEGF-
C156S (n=6 mice) or concomitantly treated with VEGF-C156S (VEGF-C) and LYVE-1 function
blocking antibody (VEGF-C+LYVE-1 Ab) (n=6 mice) from day 20. Animals receiving isogeneic
(n=3 mice) or allogeneic lung grafts were sacrificed 30 days after transplant together with age-
matched untransplanted controls (n=6 mice).
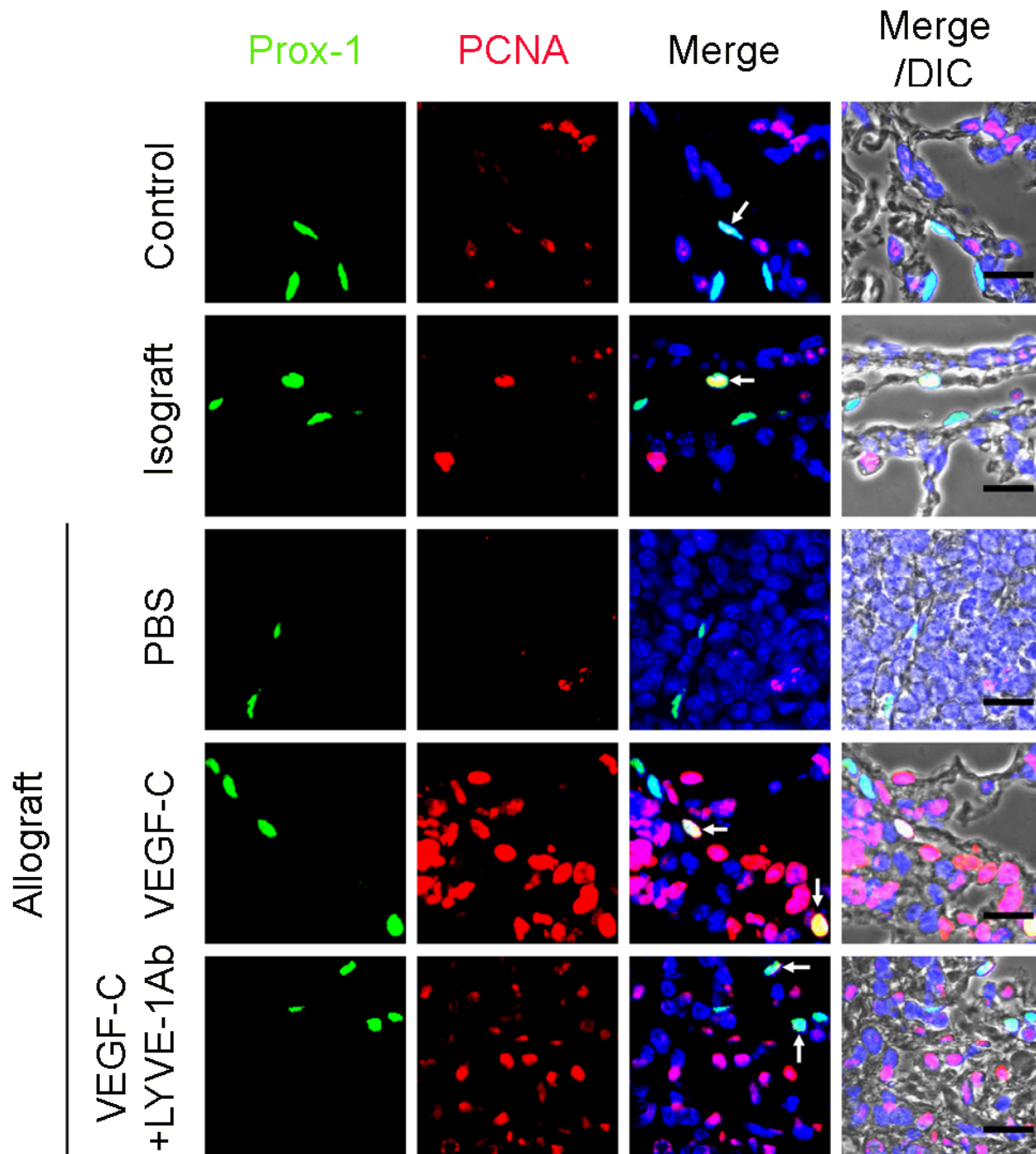
1
2  **Supplemental Figure 12 (higher magnification of images in Figure 4). VEGF-C156S**
3  **treatment stimulates lymphatic endothelial cell proliferation in lung allografts.**
4  Representative images of PROX1 (green) and proliferating cell nuclear antigen (PCNA) (red)
5  double immunofluorescence staining. PROX-1/PCNA-double positive cells are indicated by
6  white arrows. Nuclei were counterstained with DAPI (blue). Scale bars, 20µm. Animals
7  receiving allogeneic lung grafts were treated with PBS (n=5 mice), VEGF-C156S (VEGF-C)
8  (n=6 mice) or concomitantly treated with VEGF-C156S and LYVE-1 function blocking antibody
9  (VEGF-C+LYVE-1 Ab) (n=6 mice) from day 20. Animals receiving isogeneic (n=3 mice) or
10 allogeneic lung grafts were sacrificed 30 days after transplant together with age-matched
11 untransplanted controls (n=6 mice).

| CD3 | Immunohistochemistry | Catalog no. ab5690 (Abcam, Cambridge, MA) |
|-----|---------------------|-------------------------------------------|
| CD68 | Immunohistochemistry | Catalog no. ab125212 (Abcam) |
| CD68 | Immunofluorescence | Catalog no. MCA1957 (AbD Serotec, Raleigh, NC) |
| D2-40 | Immunohistochemistry | Catalog no. CM266A (BioCare Medical, Concord, CA) |
| LYVE-1 | Function blocking | Catalog no. MAB2125 (R&D Systems, Minneapolis, MN) |
| LYVE-1 | Immunohistochemistry Immunofluorescence | Catalog no. 11-034 (AngioBio, Del Mar, CA) |
| PCNA | Immunofluorescence | Catalog no. 13110 (Cell Signaling Technology, Danvers, MA) |
| Prox-1 | Immunofluorescence | Catalog no. AF2727 (R&D Systems) |
| VEGFR-2 | Immunohistochemistry | Catalog no. ab51873 (Abcam) |
| VEGFR-3 | Immunofluorescence | Catalog no. 552857 (BD Biosciences, San Diego, CA) |

**Supplemental Table 1**

List of antibodies used.